Zeitschrift: Schweizerische mineralogische und petrographische Mitteilungen = Bulletin suisse de minéralogie et pétrographie

Band: 78 (1998)

Heft: 2

Artikel: Partial eclogitization of the Ambolten gabbro-norite, North-East Greenland Caledonides

Autor: Gilotti, Jane A. / Elvevold, Synnøve

DOI: https://doi.org/10.5169/seals-59288

SCHWEIZ. MINERAL. PETROGR. MITT. 78, 273–292, 1998

Partial eclogitization of the Ambolten gabbro-norite, North-East Greenland Caledonides

by *Jane A. Gilotti*[1] and *Synnøve Elvevold*[2]

Abstract

Partially eclogitized igneous bodies composed of gabbro, leucogabbro, anorthosite, and cross-cutting diabase dikes are well represented in the North-East Greenland Eclogite Province. A 200 × 100 meter intrusive body on Ambolten Island (78° 20' N, 19° 15' W) records a prograde transition from gabbro-norite to eclogite facies coronitic metagabbro followed by retrogression to garnet amphibolite. The body is composed of an undeformed core of coronitic gabbro-norite surrounded by hydrated margins of undeformed to strongly foliated amphibolite. Igneous plagioclase + olivine + enstatite + augite + oxides convert to eclogite facies assemblages consisting of garnet, omphacite, diopside, enstatite, kyanite, zoisite, rutile and pargasitic amphibole through several coronitic reactions. Relict cumulus plagioclase laths are replaced by an outer corona of garnet, an inner corona of omphacite and an internal region of sodic plagioclase, garnet, kyanite, omphacite and zoisite. Olivine and intercumulus pyroxene are partly replaced by metamorphic pyroxenes and amphibole. The corona structures, zoning patterns, diversity of mineral compositions in a single thin section, and preservation of metastable assemblages are characteristic of diffusion-controlled metamorphism. The most extreme disequilibrium is found in static amphibolites where igneous pyroxenes, plagioclase domains with eclogite facies assemblages, and matrix amphibole coexist. Complete eclogitization was not attained at Ambolten due to a lack of fluids needed to drive diffusion during prograde and retrograde metamorphism. The P-T conditions of the high-pressure metamorphism are estimated at ≥ 750 °C and > 18 kbar. Well-equilibrated, foliated amphibolites from the margin of the gabbro-norite formed at 640–670 °C and 12.5–13.5 kbar. Eclogitization of intrusive bodies like the Ambolten gabbro-norite supports our contention that the entire North-East Greenland Eclogite Province experienced Caledonian high-pressure metamorphism, even though no eclogite facies assemblages have been found in the quartzofeldspathic host gneisses to date.

Keywords: eclogite, disequilibrium, corona, mineral zoning, Greenland Caledonides.

Introduction

Relicts of igneous rocks with varying bulk compositions can persist through eclogite facies metamorphism in dry, low-strain environments. Mafic protoliths such as gabbros and dolerites are the most robust (CHINNER and DIXON, 1973; MØRK, 1985a, 1985b, 1986; POGNANTE, 1985; INDARES, 1993; INDARES and RIVERS, 1995; ZHANG and LIOU, 1997), but granitoids can also survive (OBERHÄNSLI et al., 1985; KOONS et al., 1987; BIINO and COMPAGNONI, 1992). Older metamorphic terrains, comprised of dry granulite facies rocks such as the Bergen Arcs of Norway (e.g. AUSTRHEIM and GRIFFIN, 1985; AUSTRHEIM, 1987; JAMTVEIT et al., 1990), also show evidence of partial metamorphism to eclogites. These partly eclogitized rocks are characterized by textural and mineralogical disequilibrium that can provide useful information on the reaction paths that lead to eclogite formation (RUBIE, 1990). They contrast sharply with well-equilibrated eclogites which are more useful for geochronology and quantifying P-T conditions.

If partly eclogitized igneous relicts manage to escape deformation and subsequent retrograde recrystallization, they can preserve a rare record of the early metamorphic history. Not only can the

[1] Geological Survey, New York State Museum, State Education Department, Albany, NY 12230, USA. <jgilotti@museum.nysed.gov>

[2] Geological Survey of Denmark and Greenland, Thoravej 8, DK-2400 Copenhagen NV, Denmark. <sel@geus.dk>

protolith be recognized and characterized, but spatial information can also be discerned. This is particularly important in continent-continent collision type eclogite terrains where the high-pressure rocks are typically found as mafic lenses with strongly deformed margins enveloped by amphibolite facies, quartzofeldspathic gneisses. Survival of these common intrusive rocks (e.g. dikes, gabbros, and granites) is strong evidence that their country rocks, i.e. the gneisses, also experienced eclogite facies conditions; and that entire slabs of continental crust were subducted to depths in excess of 50 km (e.g. GRIFFIN and CARSWELL, 1985; MØRK, 1985a, 1986; INDARES, 1993) or more (ZHANG and LIOU, 1997). The fact that some igneous and metamorphic relicts are only partly eclogitized demonstrates that continental crust can exist metastably at high-P without converting to eclogite.

Numerous partially eclogitized igneous bodies have recently been discovered in the North-East Greenland Eclogite Province. The gabbro-norite on the island of Ambolten is a particularly well-exposed example of how relict igneous minerals and textures are replaced by high-pressure assemblages through several coronitic reactions. This paper describes the textures, mineral chemistry, major element zoning, and the sequence of reactions recorded by the gabbro-norite. Although emphasis is placed on the high-pressure parageneses, we also discuss the amphibolite facies overprint.

Geologic setting

The North-East Greenland Eclogite Province of the crystalline hinterland of the Greenland Caledonides (Fig. 1a) contains relict eclogites and related high-pressure rocks (GILOTTI, 1993, 1994). The province extends for approximately 400 km along strike, from Holm Land in the north to the Dove Bugt region in the south. Gray, banded, amphibolite-facies orthogneisses form the bulk of the eclogite-bearing crystalline complexes (HULL et al., 1994). The gray gneisses are dominated by 1.8–2.0 Ga calc-alkaline batholiths that were deformed and metamorphosed in the Early Proterozoic (KALSBEEK et al., 1993). These were intruded by 1.75 Ga granitoids and by later dike swarms; the entire package was then deformed and metamorphosed during the Caledonian orogeny (HULL et al., 1994). Layers and lenses of intermediate to mafic rocks with relict eclogite facies assemblages are overprinted to varying degrees by the subsequent regional amphibolite facies metamorphism. Isotopic dating has shown that the eclogite facies metamorphism seen in mafic and intermediate rocks in the North-East Greenland Eclogite Province is Caledonian in age (BRUECKNER et al., 1998).

The eclogite facies rocks occur in a variety of settings including: isolated lenses, strings of lenses, tabular bodies and layers within the quartzofeldspathic gneisses. The protoliths of the eclogites can be recognized when the rocks occur in macroscopic low strain augen. For example, some eclogites were clearly xenoliths of mafic material within the calc-alkaline batholiths; others were mafic dikes. The eclogitic rocks span a range of compositions. Eclogites *sensu stricto* (including kyanite-eclogites and bimineralic eclogites), garnet-clinopyroxenites, garnet-websterites and websterites are the most common lithologies. Garnet-clinopyroxene thermometry in bimineralic eclogites and two pyroxene thermometry in garnet websterites in the southern part of the NEGEP (77–78° N) yield regional temperatures in the range of 650–790 °C (GILOTTI, 1993, 1994; BRUECKNER et al., 1998), typical of medium temperature eclogites formed in continent-continent collisions (CARSWELL, 1990).

Numerous partially eclogitized, igneous bodies were found north of 78° N during fieldwork conducted in 1994 and 1995 under the auspices of the Geological Survey of Denmark and Greenland's Eastern North Greenland expedition. These igneous relicts are particularly abundant between 78–79° N on the islands in Jøkelbugten (Fig. 1b). The igneous rocks consist of gabbros, leucogabbros, anorthosites and diabase dikes that have been incompletely re-equilibrated in the eclogite facies. The plutons are preserved in the basement gneisses as lenticular augen, commonly 100 to 500 m long. The interior parts of the lenses contain massive, undeformed rocks that appear to retain their igneous texture and mineralogy; however, closer examination shows that they are distinctly coronitic. Except for some cross-cutting dikes, intrusive contacts are strongly deformed and always concordant with the surrounding gneissosity.

The gabbros, leucogabbros and anorthosites are thought to belong to a single intrusive suite based on field relations, but confirming geochemical or isotopic evidence does not exist at this time. Gabbros to anorthosites are widespread within the basement of the Caledonian fold belt. A Sm–Nd model age of 2146 Ma has been obtained from a gabbro-anorthositic rock located west of Bessel Fjord at 76° N (STECHER and HENRIKSEN, 1994), just south of the North-East Greenland Eclogite Province. If the partly eclogitized gabbros to anorthosites in the Jøkelbugt area belong

to the same intrusive suite as the dated sample, then these rocks were part of the Early Proterozoic crust.

Field relations

The Ambolten gabbro-norite is located at the northern high point on the island of Ambolten. UTM coordinates are zone 27 WG389964. The locality is easily recognized as two massive, brown-weathering lumps that are approximately 20 m higher than their surroundings (Fig. 2a). The gabbro-norite outcrops as a 210 × 100 meter, tadpole-shaped body that is enveloped by the host gneisses (Fig. 3). Coarse-grained, homogeneous, coronitic gabbro-norite occupies the center of the lens. Magmatic rhythmic layering, defined by dm scale modal variation of plagioclase and mafic minerals, can be seen in the northwest corner of the body (Fig. 2b). A mafic dike, now a garnet amphibolite, cuts the gabbro-norite at its southern end (Fig. 3). Only one thin shear zone was observed within the gabbro-norite at sample 434391. All sample numbers refer to files of the Geological Survey of Greenland, now incorporated into a Geological Survey of Denmark and Greenland database.

The outer margin of the gabbro-norite is amphibolitized; the width of this hydrated zone varies from 1 to 20 m. The transition from unfoliated, coronitic gabbro-norite to amphibolite is gradual, on the order of tens of centimeters. In places the amphibolitic overprint is static; for ex-

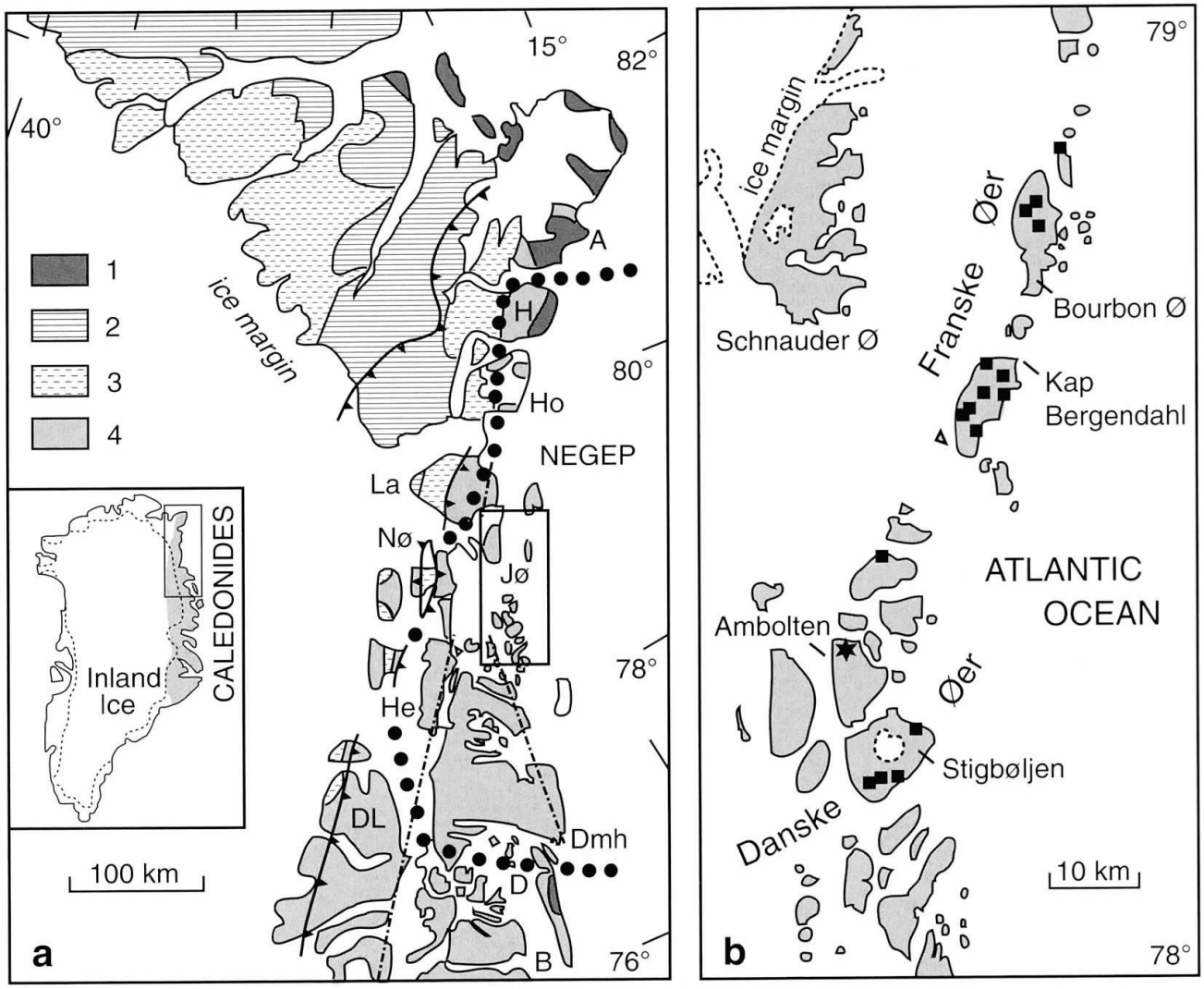

Fig. 1 (a) General geologic map of the North-East Greenland Caledonides. Major geologic units are: 1. Carboniferous basins; 2. Late Proterozoic to Silurian sedimentary sequences; 3. Middle Proterozoic sedimentary and basalt sequences; 4. Precambrian gneiss complexes, including the North-East Greenland Eclogite Province (NEGEP). A: Amdrup Land; H: Holm Land; Ho: Hovgaard Ø: Jø Jøkelbugten; La: Lambert Land; Nø: Nørreland Window; He: Hertugen af Orléans Land; DL: Dronning Louise Land; Dmh: Danmarkshavn; D: Dove Bugt; B: Bessel Fjord. (b) The Ambolten gabbro-norite locality is marked by a star; other partially eclogitized bodies (gabbros, leucogabbros, anorthosites and dikes) are indicated by squares.

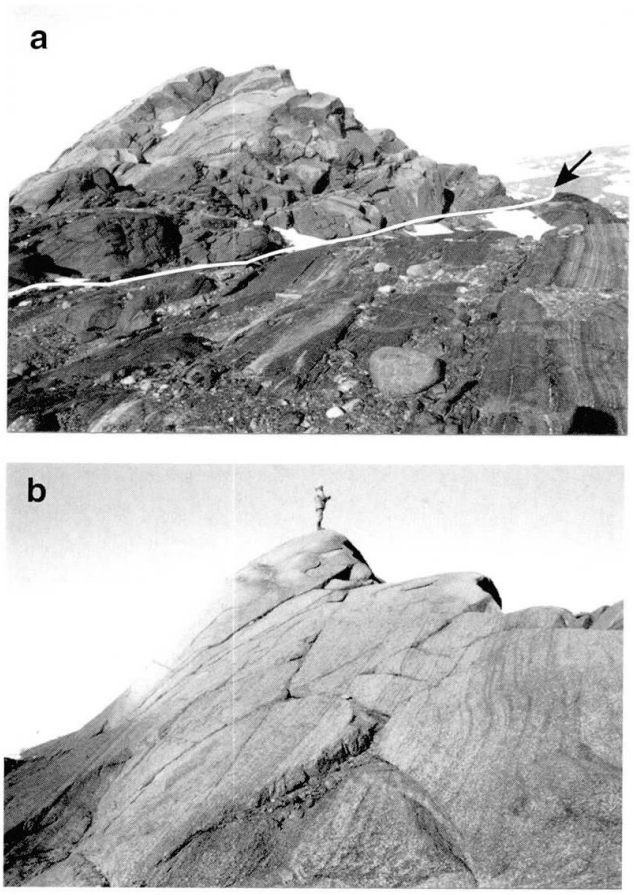

Fig. 2 (a) The SE contact (white line) between the Ambolten gabbro-norite and gneisses in the foreground. (b) Relict igneous layering on the western margin of the gabbro; the dark area in the lower left is the amphibolite margin.

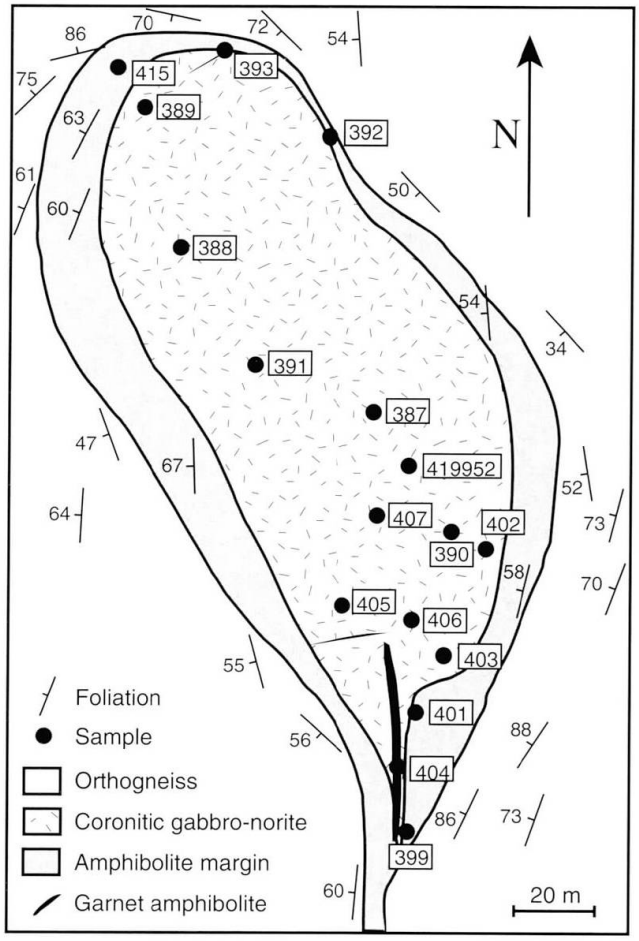

Fig. 3 Geologic map of the Ambolten gabbro-norite with sample locations shown. All sample numbers have the prefix GGU 434, except GGU 419952.

ample, igneous layering can still be seen in the amphibolitized northwest margin (Fig. 2b). More commonly, the margin is a strongly foliated amphibolite schist clearly derived from progressive deformation and metamorphism of the gabbro-norite. Deformed amphibolite is everywhere in contact with the host gneiss, and the schistosity is parallel to the foliation in the host rocks (Fig. 3). The gabbro-norite contains a few meter thick zones of garnet-amphibolite, perpendicular to the margin of the body, that were probably fractures and fluid pathways during the eclogite through amphibolite facies metamorphism.

The gray gneisses surrounding the gabbro-norite are felsic to intermediate amphibolite facies rocks. The predominant mineral assemblage is quartz + plagioclase + garnet + hornblende + biotite ± muscovite + epidote/clinozoisite + rutile ± titanite. Modal mineralogy varies from layer to layer with bulk composition. Migmatites are common in these gneisses; some of the leucosomes are oriented parallel to the axial surfaces of outcrop scale folds. Small, scattered, cm-scale, greenschist facies deformation zones cut the gneisses. These consist of fine-grained quartz + feldspar + biotite surrounding porphyroclasts of feldspar, epidote, and amphibole. The gray gneisses are also the host of well-equilibrated eclogites, some of which lie within a few hundred meters of the gabbro. Omphacite + garnet + rutile ± quartz assemblages occur in both cross-cutting mafic dikes and concordant mafic layers that probably were dikes.

Textures and mineralogy

The eclogite facies transformation failed to reach completion and the high-pressure assemblages are present as inclusion suites, in reaction rims and coronas. The original magmatic textures and relicts of the original minerals are well preserved. The most pristine igneous minerals are pyroxenes and olivine. Plagioclase is always altered and appears cloudy due to minute inclusions of kyanite, corundum, omphacite and clinozoisite. Samples that appear fresh in outcrop show extensive coro-

Tab. 1 Sample classification according to textural stages.

Stage	Figure	Sample
Magmatic	4a	
Coronitic (early)	4b	434387, 434405, 434407
Coronitic (late)	4c	419952, 434388, 434389
Static amphibolitization (early)	4d	434390, 434392, 434406
Complete recrystallization (late)	4e	434402, 434403
Deformed amphibolite		434399, 434401, 434404, 434415

nitic development when examined with an optical microscope. In rocks with the smallest degree of reaction, metamorphic phases constitute approximately 20% of the mode. The grain size of the reaction products and the width of the coronas in these rocks are very small, often < 0.05 mm. At advanced stages of transformation, the modal amount of garnet and amphibole increases while the modal amount of plagioclase and pyroxene (igneous and metamorphic) decreases.

The incomplete reaction makes it possible to unravel the reaction sequence. We have divided the textural and mineralogical development of the gabbro-norite into three sequential stages: (i) a relict igneous stage, (ii) a coronitic stage, and (iii) an amphibolite stage. In addition to these three stages, a weak but pervasive greenschist facies overprint is observed. Figure 4 is a schematic representation of the reaction history and typical textures developed during the metamorphic evolution of the Ambolten gabbro-norite, and table 1 is a classification of all the samples according to this scheme.

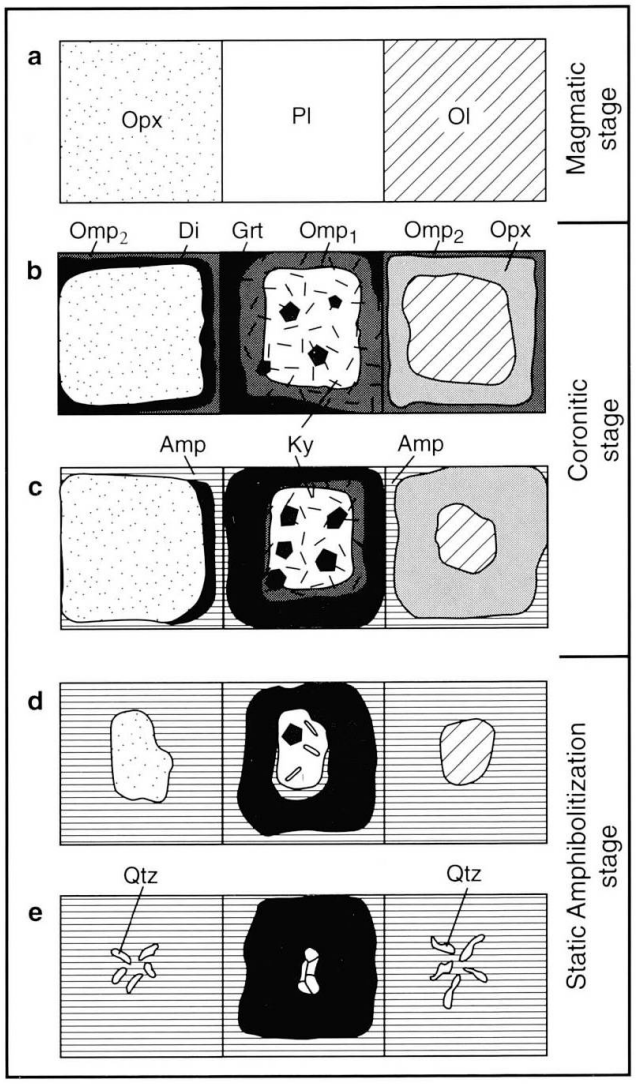

Fig. 4 Schematic reaction sequence diagram showing the textural and mineralogical evolution of the gabbro-norite.

RELICT IGNEOUS STAGE

Partial preservation of igneous minerals and textures is ubiquitous within the central core of the gabbro-norite. The least altered samples have an isotropic, coarse-grained igneous texture composed of cumulus plagioclase laths and olivine, intercumulus enstatite and augite, and ilmenite and biotite as minor phases (Fig. 5a). Olivine is sometimes included within the larger pyroxene grains. Igneous orthopyroxene and clinopyroxene are easily distinguished because the grains contain a very fine dust of oxide. The oxides were most like-

Tab. 2 Bulk rock chemistry.

Sample	419952
SiO_2	46.40
TiO_2	0.79
Al_2O_3	13.17
FeO_{total}	14.00
MnO	0.16
MgO	15.62
CaO	6.58
Na_2O	1.93
K_2O	0.62
P_2O_5	0.31
Volatiles	0.16
Total	99.74

ly exsolved from the primary pyroxenes during cooling from magmatic temperatures. Metamorphic phases are present as very thin, 0.05–0.10 mm wide coronas. No unaltered igneous plagioclase exists, but lath shapes and Carlsbad twins are preserved. The bulk geochemistry (Tab. 2) and normative mineralogy are consistent with a gabbro-norite composition.

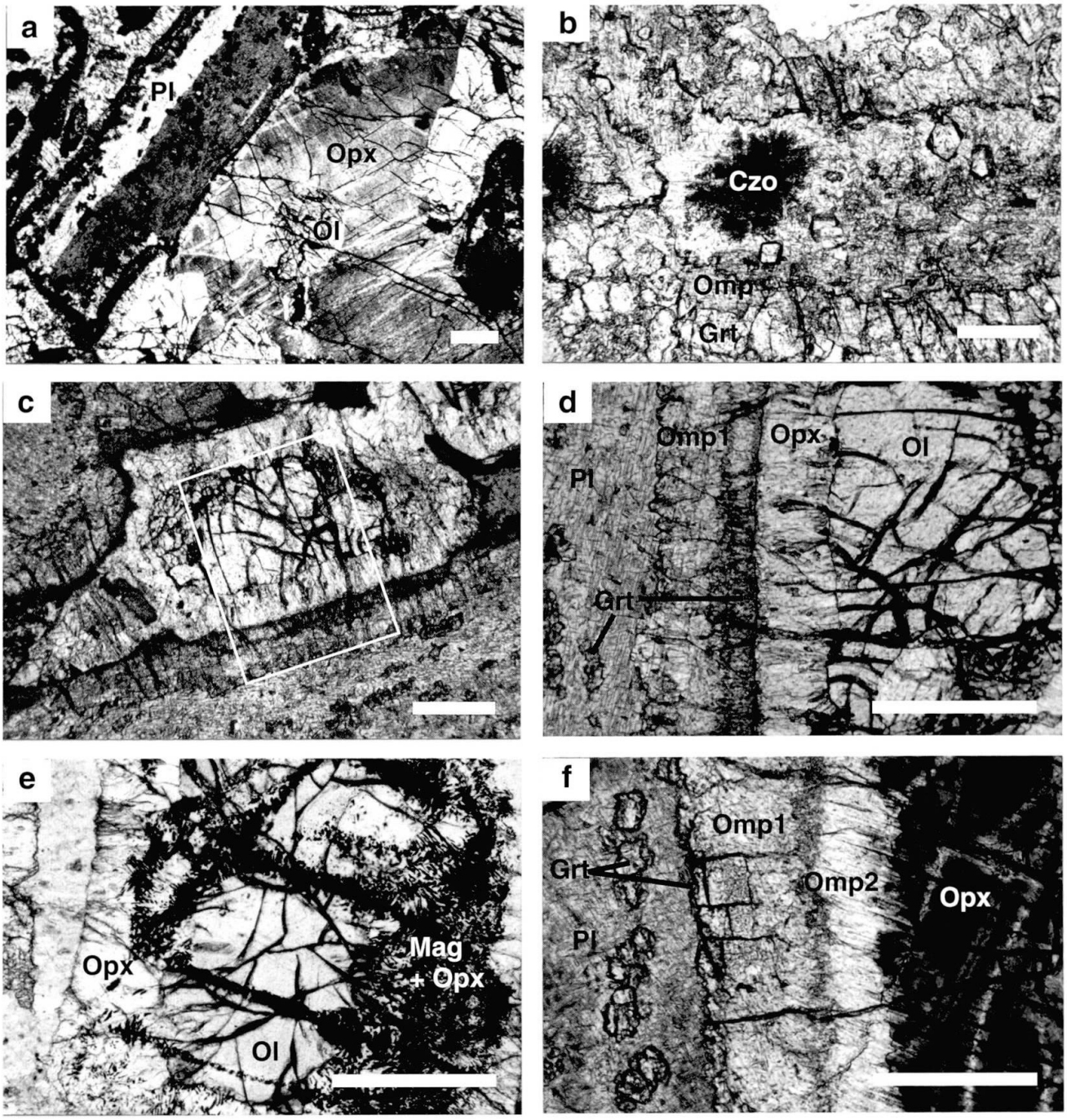

Fig. 5 Photomicrographs of the coronitic stage. Scale bars are 0.5 mm; a is crossed polarized light, and b–f are plane polarized light. (a) Well-preserved igneous texture showing olivine included in dusty orthopyroxene. Plagioclase retains its igneous lath shape and Carlsbad twins, although enclosed by a corona of garnet (black). Sample 434387. (b) High pressure assemblage is best seen in the plagioclase domains. Euhedral garnets together with kyanite and clinozoisite needles cloud the remaining plagioclase which is surrounded by a double corona of omphacite and garnet. Sample 419952. (c) A corona of fibrous orthopyroxene replaces olivine in 434387. The box outlines the area shown in (d). Complex coronas developed between the igneous plagioclase and olivine. The original phase boundary was located at the present garnet-orthopyroxene interface. (e) Intergrowths of magnetite and orthopyroxene replace olivine. Sample 419952. (f) Corona developed between igneous plagioclase and orthopyroxene. The interface between omp_1 and omp_2 marks the original phase boundary. Sample 434387.

CORONITIC STAGE

Evidence for high-pressure metamorphism is seen in complex coronas around and pseudomorphs of the original igneous minerals (Fig. 4b). Plagioclase is the reaction site of the most obvious high-pressure assemblage. All plagioclase grains are crowded with kyanite and clinozoisite needles (Fig. 5b). Corundum inclusions were noted in one sample. An inner corona of omphacite surrounds the plagioclase grains in the least reacted rocks (Fig. 4b). A few garnets nucleate in the centers of the plagioclase, but most garnet is found in an ubiquitous outer corona around the plagioclase laths (Fig. 4 b, c and Fig. 5 a, b). The omphacite and garnet both include needles of kyanite and zoisite (Fig. 4 b, c) and the garnet contains inclusions of omphacite. Rarely does omphacite completely replace any one plagioclase lath, and never is all the plagioclase in the rock consumed by the eclogite facies reactions.

Olivine is always mantled or pseudomorphed by orthopyroxene (Fig. 4 b, c and Fig. 5 c, d, e). Thin collars of radiating orthopyroxene crystals grow around olivine grains during the early stages of metamorphism. The collars grow from the outside in with additional rings of crystals added until olivine is completely consumed. In olivine grains that share a phase boundary with a plagioclase domain, an outer corona of omphacite sometimes appears around the orthopyroxene corona (Fig. 4b and Fig. 5d). Olivine exhibits cracks which are filled with very fine intergrowths of orthopyroxene and oxide (Fig. 5e). At advanced stages of transformation, olivine is the first relict phase to be completely consumed in the eclogite facies reactions.

Relict clinopyroxene recrystallizes to a fine-

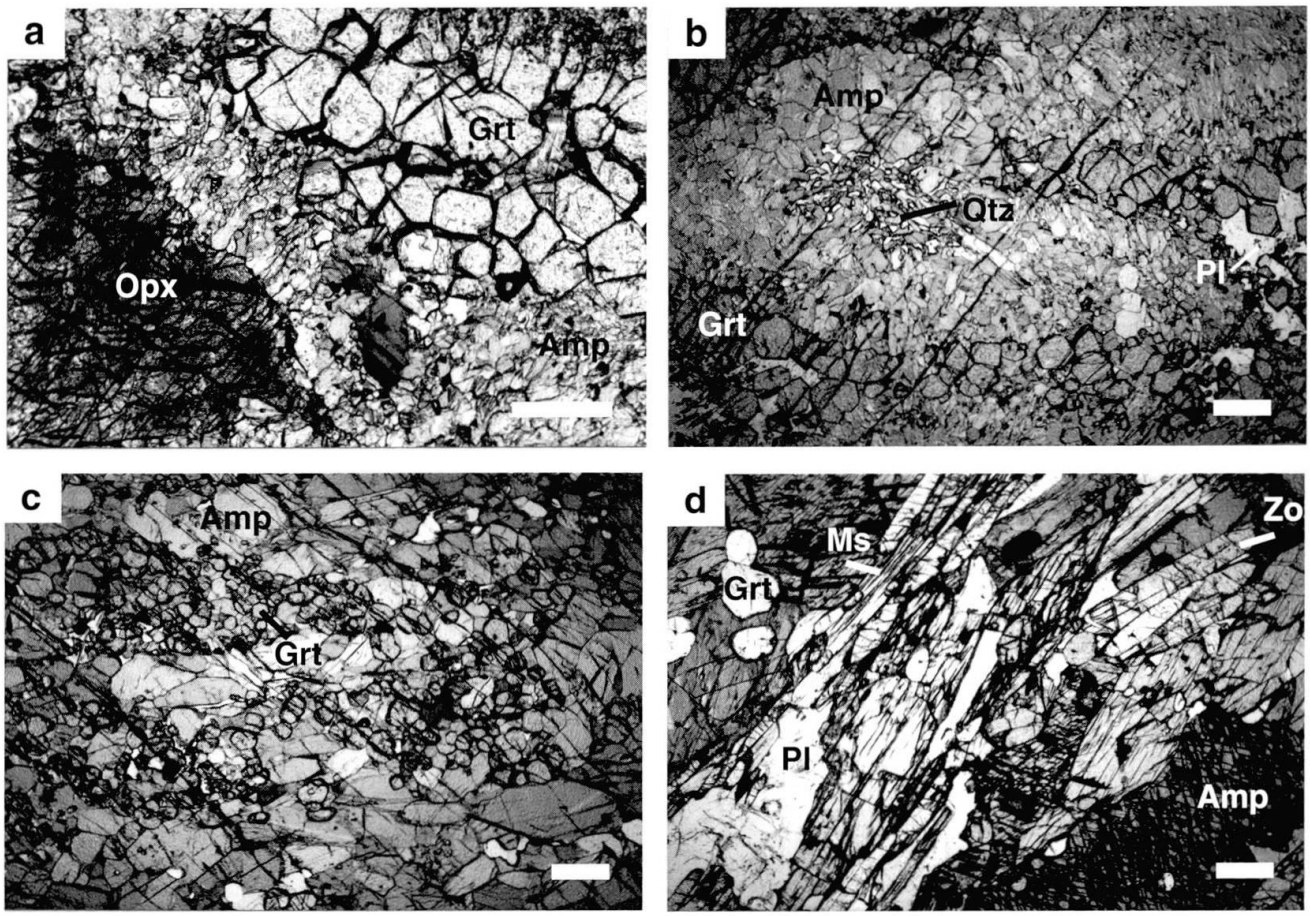

Fig. 6 Photomicrographs of the amphibolites. Scale bars are 0.5 mm; all photos are plane polarized light. (a) Undeformed amphibolites contain the most disequilibrium assemblages. Here igneous orthopyroxene coexists with HP garnet (note kyanite inclusions) and fine-grained pargasitic- to magnesio-hornblende. Sample 434406. (b) Amphibole progressively consumes the HP pyroxenes, while garnet pseudomorphs mark former plagioclase domains. The remaining plagioclase is clear and recrystallized. Sample 434390. (c) A weak foliation is defined by elongated clumps of garnet aggregates and aligned amphibole grains. Even in these low strain samples, the garnet aggregates still identify the original plagioclase domains. Sample 434401. (d) An equilibrium texture is finally obtained in the strongly foliated and most hydrated amphibolites along the margin of the gabbro. Sample 434415.

grained mass of new grains which are oxide free. Relict orthopyroxene is initially surrounded by a corona of metamorphic diopside (Fig. 4b). A second (outer) corona of omphacite may form in grains that share a boundary with plagioclase. In a few cases, a thin, outermost corona of biotite was observed.

Small amounts of pale green, fine-grained, early amphibole are found associated with the garnet and omphacite coronas around plagioclase, and are interpreted to be part of the high-pressure assemblage. Ilmenite is often surrounded by red brown biotite.

AMPHIBOLITE STAGE

Amphibolitization is most pronounced at the margin of the body (Fig. 3), although trace amounts of secondary amphibole are found in all the samples. The first minerals to be replaced by amphibole are omphacite and coronal diopside (Fig. 4 b, c). Metamorphic orthopyroxene pseudomorphs after olivine and igneous pyroxenes still persist at the early stage of amphibolite formation. With progressive hydration, the modal amount of garnet and amphibole increases at the expense of plagioclase and pyroxenes (Fig. 4d and Fig. 6a). Pyroxene is finally consumed by amphibole, with or without biotite, while garnet replaces plagioclase (Fig. 4e). In low strain areas, clusters of garnet and amphibole still mimic primary mineral domains (Fig. 6b). Remaining plagioclase recrystallizes to large, clean grains devoid of kyanite and zoisite needles. Rutile develops overgrowths of titanite, and is eventually consumed. Quartz often occurs as small blebs in the central parts of the amphibole domains (Fig. 4e and Fig. 6b). Further recrystallization involves grain boundary migration and grain coarsening.

Up to this point, the amphibolites we have described are massive, unfoliated rocks that were evidently metamorphosed in a static environment. However, deformed amphibolites derived from the gabbro exist everywhere along its outer margin. The typical assemblage is garnet + amphibole + quartz ± plagioclase + biotite + titanite ± epidote/clinozoisite. Low strain amphibolites contain lens-shaped clumps of small, recrystallized, inclusion-free garnet grains that are flattened parallel to a planar fabric (Fig. 6c). Preferred orientations of blocky amphibole grains and less abundant biotite laths also help define the planar fabric. Quartz and plagioclase occur as polygonal grains in the groundmass together with amphibole and biotite. In more highly strained samples, the clumps of garnets disperse into a more homogeneous and well equilibrated distribution of phases (Fig. 6d). One sample of amphibolite schist (434415) has the assemblage garnet + amphibole + zoisite + plagioclase + quartz + white mica.

Tab. 3 Relict igneous mafic phases.

Mineral	Ol	Opx	Aug
Sample	434407	434387	434387
Point	17	13	46
SiO_2	38.23	54.07	53.13
TiO_2	0.00	0.59	0.52
Al_2O_3	0.00	0.91	2.45
FeO	24.49	15.87	6.06
MnO	0.23	0.18	0.07
MgO	38.54	28.26	16.04
CaO	0.00	0.22	20.15
Na_2O	0.00	0.03	1.21
K_2O	0.00	0.00	0.00
Cr_2O_3	0.00	0.00	na
NiO	0.03	0.00	na
$Wt\%_{tot}$	101.52	100.14	99.62
Si	0.989	1.941	1.944
Al^{IV}	0.000	0.039	0.056
Al^{VI}	0.000	0.000	0.049
Fe^{3+}	0.000	0.050	0.065
Ti	0.000	0.016	0.014
Cr^{3+}	0.000	0.000	0.000
Mg	1.486	1.512	0.874
Fe^{2+}	0.530	0.426	0.120
Mn	0.005	0.006	0.002
Ca	0.000	0.009	0.790
Na	0.000	0.002	0.086
%Ca	0.00	0.45	42.67
%Mg	73.71	75.48	47.23
%Fe	26.29	24.07	10.10

LOW TEMPERATURE ALTERATION

Greenschist facies minerals are volumetrically small, but pervasive in the rocks. Quite a few samples are cut by very narrow, parallel, transgranular fractures which are lined with carbonate, chlorite, and/or opaques. Chlorite and carbonate fill voids, and chlorite pseudomorphs after garnet are observed in one sample. The fractures cut across the amphibolite facies foliation, and seem to be the pathway for fluids of a more CO_2 rich composition.

Mineral chemistry

Representative chemical analyses of minerals in their various textural settings are given in tables 3–7. Pyroxene nomenclature follows MORIMOTO

Tab. 4 Metamorphic clinopyroxene.

Mineral	Omp 1	Omp 1	Omp 1	Omp 2	Omp 2	adjacent to Opx		Omp rim	Incl. in grt
Sample	434387	434407	419952	434388	434406	434407	434387	434394	434409
Point	4	7	34	27	6	13	17	23	41
SiO_2	54.65	52.32	54.62	55.88	54.42	54.98	54.41	52.85	54.05
TiO_2	0.28	0.22	0.14	0.02	0.10	0.23	0.05	0.21	0.18
Al_2O_3	17.72	16.08	16.80	8.88	6.39	3.12	2.13	8.19	8.59
FeO	3.81	3.67	3.58	4.58	5.29	4.91	6.02	6.47	5.02
MnO	0.00	0.03	0.00	0.00	0.04	0.11	0.13	0.05	0.08
MgO	5.54	7.08	5.99	10.52	11.36	14.16	14.21	10.50	11.01
CaO	10.96	15.03	10.72	14.93	16.96	20.66	20.73	17.86	17.50
Na_2O	8.50	6.59	8.75	5.97	4.82	2.65	2.20	4.40	3.30
K_2O	0.00	0.00	0.00	0.00	0.00	0.00	0.00	0.00	0.02
Cr_2O_3	na	0.01	na	0.00	0.23	0.19	0.01	0.06	na
NiO	na	0.00	na	0.00	0.00	0.00	0.00	na	na
$Wt\%_{tot}$	101.45	101.04	100.60	100.79	99.61	100.99	99.89	100.59	99.74
Recalculated mineral formulas (MORIMOTO et al., 1988):									
Si	1.894	1.837	1.902	1.970	1.959	1.972	1.983	1.895	1.964
Al^{IV}	0.106	0.163	0.098	0.030	0.041	0.028	0.017	0.105	0.036
Al^{VI}	0.618	0.501	0.591	0.339	0.230	0.104	0.074	0.242	0.331
Fe^{3+}	0.045	0.098	0.090	0.098	0.134	0.092	0.096	0.155	0.000
Ti	0.007	0.006	0.004	0.000	0.003	0.006	0.001	0.006	0.005
Cr^{3+}	0.000	0.000	0.000	0.000	0.007	0.005	0.000	0.002	0.000
Mg	0.286	0.370	0.311	0.554	0.610	0.757	0.772	0.561	0.596
Fe^{2+}	0.066	0.010	0.014	0.037	0.025	0.055	0.087	0.039	0.152
Mn	0.000	0.001	0.000	0.000	0.001	0.003	0.004	0.002	0.002
Ca	0.408	0.565	0.400	0.564	0.654	0.794	0.810	0.687	0.681
Na	0.571	0.448	0.591	0.408	0.336	0.185	0.156	0.306	0.233
End members for Ca–Na pyroxenes:									
Q	39.94	51.32	38.02	58.61	65.71	81.31	84.27	67.79	75.45
Jd	56.56	42.41	54.79	32.69	22.92	11.00	7.66	22.25	24.55
Ae	3.51	6.27	7.18	8.70	11.37	7.69	8.07	9.95	0.00

et al. (1988); amphibole nomenclature is after LEAKE et al. (1997). Minerals were analyzed at the Department of Earth and Environmental Sciences, Rensselaer Polytechnic Institute, Troy, New York with a JEOL 733 microprobe operated with five spectrometers in WDS mode at 15 kV accelerating voltage, and a beam current of 15 nA. A ZAF correction was applied to the data. Forty-five X-ray maps were collected for detailed study of chemical zoning in metamorphic and relict igneous phases. The X-ray maps were obtained by moving the microprobe stage in a rectangular grid pattern under a fixed beam (current approximately 200 nA) and collecting X-ray intensity data for five elements at each spot. The compositional maps, together with petrographic analysis, form the basis for interpretation of the reaction history, and were also used to locate representative spots for quantitative mineral chemistry.

IGNEOUS PHASES

The composition of the original igneous plagioclase can be estimated from the CIPW norm as bytownite (approximately An_{55-59}), but such calcic compositions are no where preserved in the analyzed samples. The most An-rich plagioclase (An_{36}) is measured in samples with the least amount of corona development. Plagioclase compositions typically range from An_{15-25} in domains where the high-pressure assemblage is well-developed. The chemical variation within any given grain is patchy; and composition becomes more sodic as Ca diffuses into sites where garnet, zoisite, or omphacite are produced.

Olivine is present in all samples with relict igneous texture and mineralogy. Its composition ranges between Fo_{72} and Fo_{79}. No intragranular chemical zoning is observed. Relict orthopyroxene and clinopyroxene appear dark and cloudy due to very fine-grained oxides. Their original composition prior to exsolution of the oxides is

Tab. 5 Garnet.

Texture	core of Pl	Grt corona Pl – center – Opx			Grt corona Pl – center – Amp			rim	rim at omp incl	core
Sample	434387	434405	434405	434405	434403	443403	434403	434394	434409	434415
Point	18	10	11	12	12	11	10	24	40	13
SiO_2	39.32	39.64	39.65	39.78	40.39	39.74	39.62	38.38	39.87	39.51
TiO_2	0.00	0.03	0.04	0.05	0.05	0.05	0.05	0.02	0.03	0.05
Al_2O_3	22.41	22.78	22.77	22.52	23.20	23.36	23.25	22.19	22.53	22.69
FeO	16.79	18.55	19.31	22.51	22.76	23.20	23.29	23.93	23.54	22.96
MnO	0.20	0.27	0.42	0.49	0.51	0.50	0.47	0.89	0.60	0.72
MgO	1.84	4.87	7.63	10.59	11.28	11.73	11.12	5.68	7.50	8.09
CaO	20.60	16.32	11.90	5.29	4.32	3.90	3.81	10.37	8.30	8.34
$Wt\%_{tot}$	101.15	102.46	101.71	101.22	102.50	102.47	101.62	101.46	102.37	102.34
Mineral formulas (12 oxygens):										
Si	3.000	2.972	2.969	2.981	2.977	2.938	2.954	2.946	2.992	2.963
Ti	0.000	0.002	0.002	0.003	0.003	0.003	0.003	0.001	0.002	0.003
Al	2.015	2.013	2.010	1.989	2.016	2.035	2.043	2.007	1.993	2.006
Fe^{2+}	1.071	1.163	1.210	1.411	1.404	1.434	1.452	1.536	1.478	1.440
Mn	0.013	0.017	0.027	0.031	0.032	0.031	0.030	0.058	0.038	0.046
Mg	0.210	0.544	0.852	1.183	1.239	1.292	1.236	0.649	0.839	0.904
Ca	1.684	1.311	0.955	0.425	0.342	0.309	0.304	0.853	0.668	0.670
X_{prp}	0.07	0.18	0.28	0.39	0.41	0.42	0.41	0.21	0.28	0.30
X_{alm}	0.36	0.38	0.40	0.46	0.47	0.47	0.48	0.50	0.49	0.47
X_{sps}	0.00	0.01	0.01	0.01	0.01	0.01	0.01	0.02	0.01	0.02
X_{gro}	0.57	0.43	0.31	0.14	0.11	0.10	0.10	0.28	0.22	0.22

not known. Analyzed orthopyroxene is rather homogenous enstatite (En_{73}–En_{77}). The clinopyroxene is sub-calcic augite and augite in samples with the least amount of corona development. Otherwise, all the clinopyroxene relicts analyzed are diopside. No zoning was observed in clinopyroxene; whereas, a slight rimward increase in Al_2O_3 is observed in orthopyroxene.

METAMORPHIC PHASES

Coronite: Metamorphic clinopyroxene shows a wide range of composition depending on its textural position. Omphacite surrounding and nucleating within plagioclase domains (Omp_1) typically has a composition in the range of Jd_{35}–Jd_{55} (Ae_5–Ae_{10}), though values as low as Jd_{18} are observed. Zoning is commonly discerned in Omp_1 with higher values of Na found near the plagioclase host (Fig. 7a). Clinopyroxene coronas around relict orthopyroxene are typically strongly zoned in Na, and omphacite may form adjacent to the plagioclase domain (Omp_2) (Fig. 7a). This omphacite is less sodic than Omp_1, rarely exceeding Jd_{30}; while the clinopyroxene adjacent to the relict orthopyroxene is typically diopside (Jd_{10}). The presence of three distinct clinopyroxenes within a single thin section is evidence of extreme chemical disequilibrium.

Colorless, fine-grained metamorphic enstatite (En_{76}–En_{80}) replaces igneous orthopyroxene and olivine, starting as coronas and ending as complete pseudomorphs with progressive reaction. The recrystallized enstatite has slightly more

Tab. 6 Plagioclase.

Mineral	highest Ca	cloudy	recrystallized		
Sample	434407	434406	434406	434403	434415
Point	39	43	27	2	17
SiO_2	58.58	61.12	64.00	65.21	63.68
Al_2O_3	26.52	23.86	22.12	21.49	22.27
FeO	0.04	0.11	0.05	0.21	0.04
CaO	7.51	4.59	2.53	1.77	3.38
Na_2O	8.07	8.88	9.95	10.61	9.72
K_2O	0.32	0.18	0.16	0.03	0.14
$Wt\%_{tot}$	101.03	98.73	98.81	99.32	99.22
Mineral formulas (8 oxygens):					
Si	2.602	2.745	2.851	2.886	2.832
Al	1.388	1.263	1.161	1.121	1.167
Fe^{2+}	0.001	0.004	0.002	0.008	0.001
Ca	0.357	0.221	0.121	0.084	0.161
Na	0.694	0.773	0.859	0.910	0.838
K	0.018	0.010	0.009	0.002	0.008

Tab. 7 Amphibole.

Texture	highest Na	Amp	lowest Al	at Opx	at Pl	core	rim	core
Sample	419952	419952	434387	434390	434390	434403	434403	434415
Point	18	13	40	1	2	8	9	2
SiO_2	42.34	40.86	41.24	50.392	46.106	48.50	48.31	44.08
TiO_2	0.21	0.33	0.33	0.237	0.583	0.73	0.56	0.39
Al_2O_3	17.78	19.20	17.05	9.445	14.597	10.98	11.28	16.62
FeO	8.25	8.10	9.12	7.127	7.83	9.54	8.44	9.96
MnO	0.01	0.04	0.01	0.028	0.061	0.07	0.04	0.05
MgO	13.93	13.23	14.73	17.403	15.187	16.14	16.91	12.82
CaO	9.86	9.57	11.23	10.374	10.066	8.67	9.21	10.12
Na_2O	4.18	3.98	2.82	2.581	3.461	3.13	3.06	2.81
K_2O	1.65	1.25	1.95	0.436	0.857	0.43	0.34	0.51
Cr_2O_3	na	0.00	na	na	na	0.00	0.00	0.00
NiO	na	0.00	na	na	na	0.00	0.00	0.00
$Wt\%_{tot}$	98.22	96.57	98.48	98.02	98.75	98.19	98.15	97.34
Mineral formulas and names based on 23 oxygens and 13 cations (LEAKE et al., 1997)								
Si	6.040	5.885	5.880	6.997	6.446	6.712	6.682	6.267
Al^{iv}	1.960	2.115	2.120	1.003	1.554	1.288	1.318	1.733
Al^{vi}	1.030	1.143	0.745	0.542	0.851	0.503	0.521	1.051
Ti	0.023	0.036	0.035	0.025	0.061	0.076	0.058	0.042
Fe^{3+}	0.415	0.606	0.739	0.553	0.474	1.104	0.976	0.649
Mg	2.962	2.840	3.131	3.602	3.165	3.330	3.487	2.717
Fe^{2+}	0.570	0.369	0.349	0.275	0.441	0.000	0.000	0.535
Mn	0.001	0.005	0.001	0.003	0.007	0.008	0.005	0.006
Ca	1.507	1.477	1.716	1.543	1.508	1.286	1.365	1.541
Na	1.156	1.111	0.780	0.695	0.938	0.840	0.821	0.775
K	0.300	0.230	0.355	0.077	0.153	0.076	0.060	0.092
Name	alumino-pargasite	alumino-magnesio-taramite	pargasite	magnesio-hornblende	pargasite	ferri-barrosite	barrosite	alumino-tschermakite

Al_2O_3 and MgO and less CaO and Na_2O than the igneous relicts.

Metamorphic garnets grow as small euhedral grains in plagioclase and as coronas surrounding the plagioclase laths. Garnets within plagioclase are strongly enriched in the grossular component (X_{grs} = 0.55–0.57). These garnets are concentrically zoned and show decreasing grossular and Fe/(Fe + Mg) from core to rim, while pyrope and almandine increase towards the rim (Fig. 8). The most grossular-rich cores show the highest values of Fe/(Fe + Mg), Fe/(Fe + Mg) = 0.80–0.84. Garnet in the necklaces mantling the plagioclase is roughly concentrically zoned with higher values of grossular and Fe/(Fe + Mg) on the plagioclase side of the corona and lower values of grossular and Fe/(Fe + Mg) towards the matrix side. Where the corona is composed of clusters of euhedral garnets, the cores of individual grains are always higher in grossular than the rims.

Amphibole is present in almost all of the Ambolten metagabbro samples, and its composition varies significantly depending on the degree of hydration and reequilibration. The early amphiboles, i.e. those that infiltrate samples that still preserve eclogite facies assemblages, are pargasite and alumino-pargasite to alumino-magnesio-taramite. These early amphiboles fill the interstices around garnet and form coronas just outside the garnets, and hence are more sodic. The amphiboles are Mg-rich with $Mg/(Mg + Fe^{2+}) \geq 0.80$–0.95, reflecting the high Mg bulk composition of the gabbro-norite. Lower Na and lower Al magnesio-hornblende is more likely to replace the metamorphic pyroxenes. These amphiboles are strongly zoned in both Al and Mg with decreasing Al and increasing Mg towards pyroxene (Fig. 9 a, b). The replacement of pyroxene by inwards extension of the amphibole means that the first amphibole to grow is a pargasitic amphibole and the later one is edenitic in composition.

Amphibolite: Garnets from the amphibolites are relatively homogenous almandine-pyrope solid solutions with less grossular than garnets from the coronitic gabbro-norite. Garnets in unfoliated amphibolites have the composition X_{alm} =

0.47–0.48, X_{prp} = 0.41–0.42, X_{grs} = 0.10–0.11, while garnets in foliated amphibolites have the composition X_{alm} = 0.47–0.50, X_{prp} = 0.28–0.30, X_{grs} = 0.19–0.22.

At the static amphibolite stage (Fig. 4 d, e), fine-grained mosaics of amphibole comprise much of the groundmass separating plagioclase relicts with garnet coronas from relict pyroxene. Al is strongly zoned in amphibole, ranging from 9.4 weight % Al_2O_3 adjacent to enstatite versus 14.6 adjacent to plagioclase (Fig. 9a). Once the amphibolite is deformed and re-equilibrated, Al is

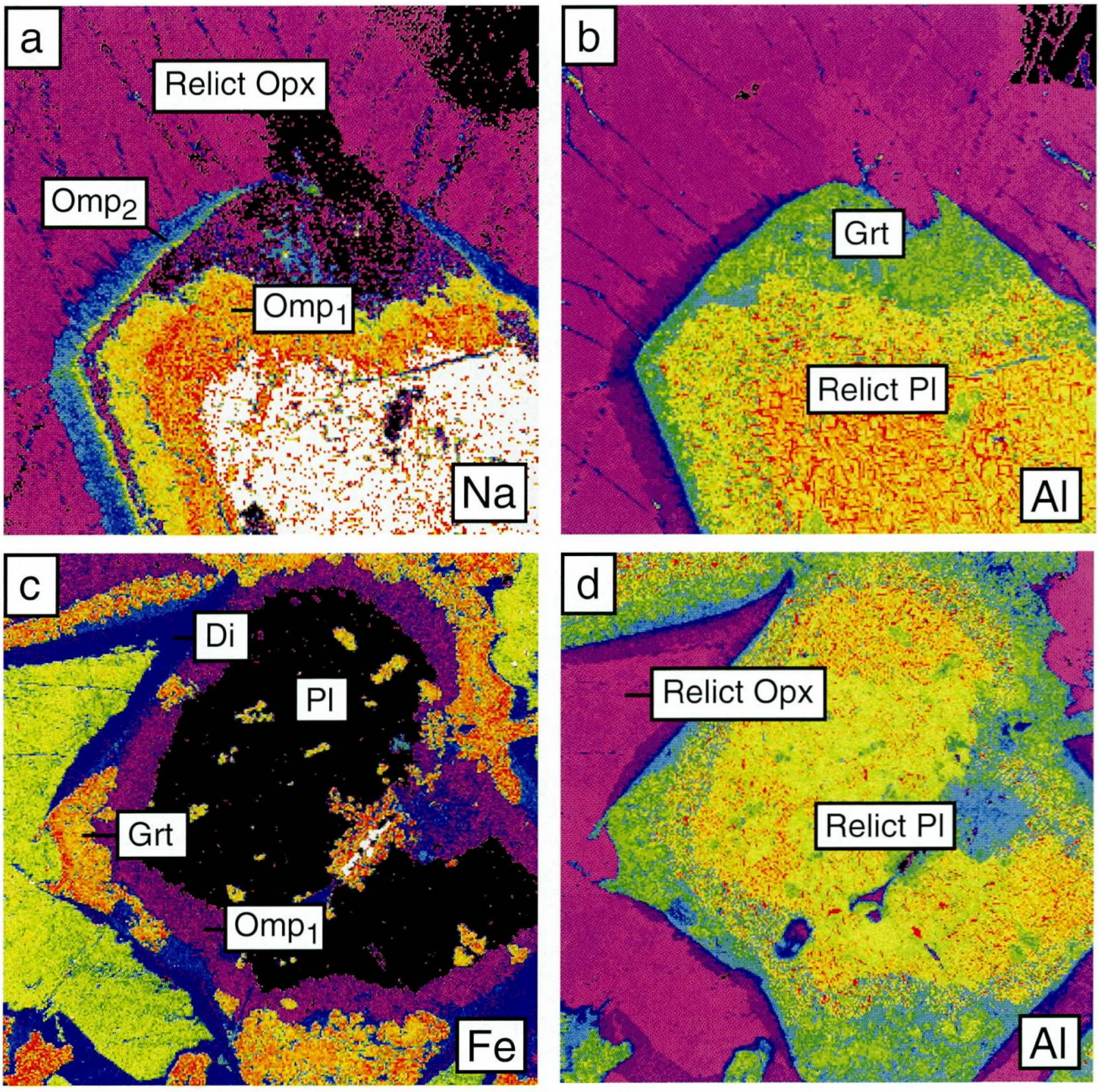

Fig. 7 X-ray maps showing compositional zoning for element in lower right. Red colors represent high concentrations and purple colors show areas of low concentration. (a) X-ray image showing the distribution of Na in a plagioclase domain and adjacent orthopyroxene. Na has diffused from the plagioclase domain into orthopyroxene to produce a 0.1 mm wide corona of omphacite (Omp_2). Precursor plagioclase has decomposed to Omp_1 and kyanite. Image is 1.6 mm wide; sample 434407. (b) Corresponding Al map shows the sharp boundary of the igneous plagioclase. Al mobility was restricted to the plagioclase domain during the coronitic stage. (c) X-ray map from 434387 showing the distribution of Fe among the magmatic and metamorphic phases. Fe (and Mg) diffuse into the plagioclase domains to reaction sites where garnet is formed. The highest concentrations of Fe occur adjacent to relict orthopyroxene. Image is 3.7 mm wide. (d) Corresponding Al distribution map defines the original igneous phase boundary between plagioclase and pyroxene.

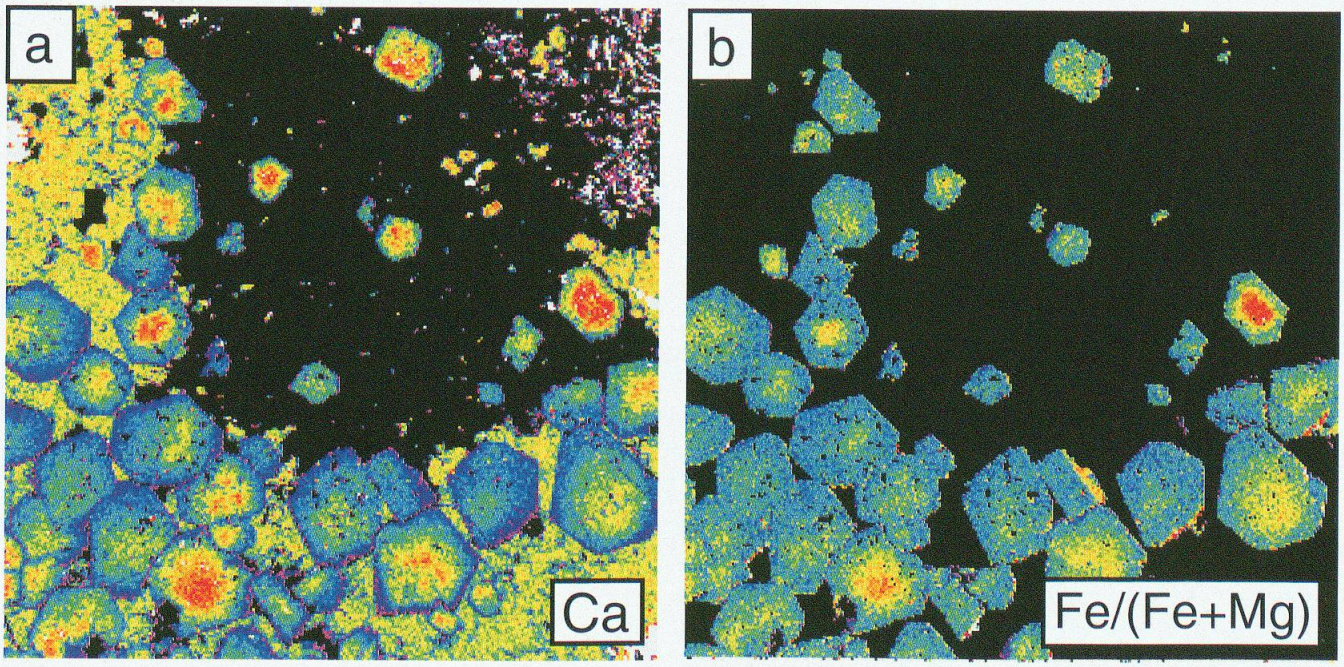

Fig. 8 X-ray maps showing the distribution of (a) Ca and (b) the Fe/(Fe + Mg) ratio in euhedral garnets crystallizing in a plagioclase domain (black). The garnets are concentrically zoned and contain a grossular rich core. The core to rim decrease in X_{grs} is 0.16 units. Fe/(Fe + Mg) shows a rimward decrease of 0.12 units. Image is 4.3 mm wide; sample 434390.

homogenized and the amphiboles fall in the tschermakite to magnesio-hornblende range.

Plagioclase begins to recrystallize during amphibolite facies hydration (Fig. 4e). Clear, polygonal grains form a mosaic adjacent to the garnet coronas. The recrystallized areas are slightly more sodic (An_{10-15}) than the inclusion-rich areas (An_{15-22}). Samples that have been deformed and completely recrystallized in the amphibolite facies contain plagioclase that is mostly oligoclase (An_{8-16}).

Chemical zoning and element mobility

Compositional zoning is most pronounced in the metamorphic corona phases, while relicts of igneous olivine, enstatite and diopside are homogenous. The spatial variation in chemical composition is demonstrated by X-ray maps (Figs 7, 8 and 9).

Figure 7a shows Na distribution maps of plagioclase domains and adjacent relict orthopyroxene. Na was for the most part redistributed within the plagioclase domains, although some Na has diffused into the relict pyroxene to form thin Na-pyroxene coronas. Figures 7b and 7d show the distribution of Al in precursor plagioclase and adjacent mafic domains. The plagioclase domain, which consists of sodic plagioclase, omphacite, kyanite and garnet, has a higher concentration of Al than adjacent mafic domains, which consist of relict orthopyroxene mantled by a thin corona of metamorphic clinopyroxene. The strong contrast in Al concentration between the mafic and plagioclase domains defines the original phase boundary between cumulus plagioclase and intercumulus pyroxenes. These Al maps clearly demonstrate that Al diffusion was confined to plagioclase domains in the least recrystallized rocks.

The distribution of Fe in igneous and metamorphic phases is shown in figure 7c. Fe and Mg were released at reaction sites along the margins of orthopyroxene that underwent $CaMg_{-1}$ and $CaFe_{-1}$ substitution during formation of metamorphic clinopyroxene, and diffused into the plagioclase domain in order to form the almandine and pyrope components of garnet and the diopside component in omphacite. The greatest volume of garnet formed along phase boundaries between plagioclase and pyroxene (especially in the corners of plagioclase domains), but some garnet nucleated at intracrystalline sites within plagioclase, requiring longer diffusion distances for Fe and Mg. In contrast to Al, Fe is much more mobile and does not define any former phase boundaries between plagioclase and pyroxene (Fig. 7c).

Isolated, euhedral garnets within the plagioclase domains are characterized by a strong core to rim decrease in grossular and a slight decrease in Fe/(Fe + Mg) (Fig. 8 a, b). This zoning pattern is interpreted as growth zonation. The Ca source for

the grossular component in garnet is the anorthite component in plagioclase. Fractionation of Ca into the core of the growing garnet shifts the bulk composition of the remaining plagioclase towards a more sodic composition. The Ca zoning in garnet is thus believed to be a result of fractional crystallization where the composition of the material supplied to the garnet rim changes with time as the garnet grows, rather than an equilibrium response to changing P-T conditions. Corona garnet mantling plagioclase is also strongly zoned with the highest grossular content nearest the plagioclase domains or as a ridge along the center part of the corona. If the first crystallizing garnet was grossular-rich as in the isolated garnets, then the corona zoning pattern implies that garnet grew from the omp_1 corona outwards to the original plagioclase phase boundary.

The most extreme disequilibrium is found in the static amphibolites where igneous pyroxenes, plagioclase domains with the high-pressure assemblages, and zoned amphiboles coexist. Amphibole fills fractures in relict pyroxenes; and amphibole coronas surround igneous pyroxenes, separating them from garnet coronas that have almost replaced the plagioclase domains. Amphiboles have the highest Al values near garnet with a systematic decrease towards pyroxene, and magmatic phase boundaries can no longer be discerned from the Al map (Fig. 9a). The highest Mg values are found adjacent to pyroxene (Fig. 9b). Al becomes somewhat mobile at this stage due to local fluid infiltration required to grow amphibole; however, the zoning still reflects a chemical gradient between the Mg-rich mafic domains and the aluminous plagioclase domains, and is thus controlled by local gradients in chemical potential rather than changing P-T conditions. Even at this stage, where a fluid has invaded the gabbro, equilibrium is not attained.

Reaction pathways

The reaction sequence is inferred from the reaction products in plagioclase domains and the different coronitic textures. Information gained from the X-ray maps has enabled us to distinguish the original phase boundaries between precursor plagioclase and mafic phases. This is particularly useful when deducing the reaction pathways and when considering element mobility between the different chemical domains.

BREAKDOWN OF OLIVINE

Two reactions describing the decomposition of olivine can be written for the coronitic metagabbros. Breakdown of olivine involving exsolution of an oxide phase occurs along fractures and phase boundaries (Fig. 5e). The observed textures can be explained by the reaction:

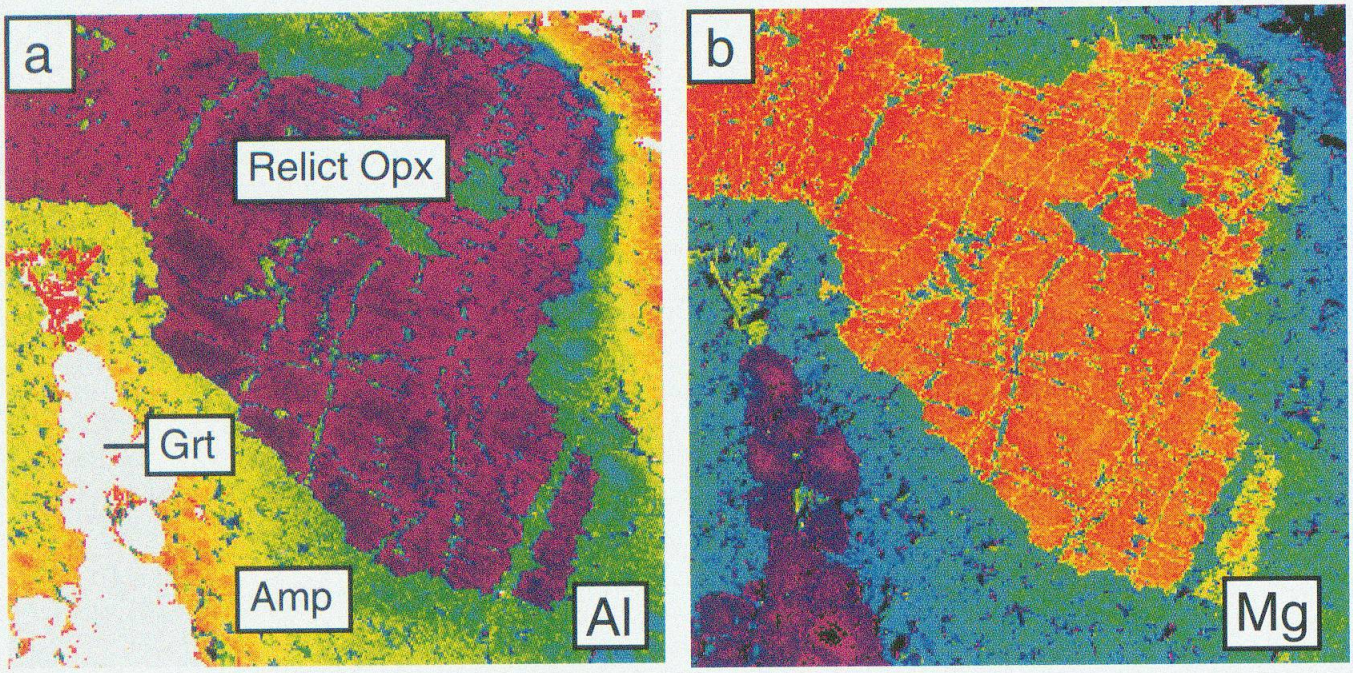

Fig. 9 (a) Al and (b) Mg compositional maps showing zoning in amphibole replacing relict orthopyroxene by inward growth of the corona. The amphibole is strongly zoned with higher values of Al_2O_3 adjacent to plagioclase domains and higher values of MgO near pyroxene. The zoning is controlled by chemical potential gradients between precursor igneous phases. Image is 3.0 mm wide; sample 434390.

$$Ol = Opx + Mag \quad (1)$$

Reaction (1) is isochemical. A second olivine breakdown reaction occurred in domains devoid of oxides. Coronas of fibrous, radial orthopyroxene (Fig. 5d) are interpreted to have formed according to the reaction:

$$Ol + Qtz = Opx \quad (2)$$

SiO_2 required for reaction (2) must have been released from the decomposition of plagioclase (see below). Quartz has not been detected within the plagioclase domains, which suggests that SiO_2 diffused from the plagioclase domains to reaction sites surrounding olivine.

BREAKDOWN OF PLAGIOCLASE

Breakdown of plagioclase, which is interpreted to be simultaneous with reactions (1) and (2), takes place along phase boundaries and at sites within the grains. Plagioclase laths are surrounded by an inner corona of very fine-grained omphacite and an outer, discontinuous and irregular corona of garnet (Fig. 5d). Smaller grains of igneous plagioclase are locally completely pseudomorphed by omphacite. Plagioclase includes abundant kyanite needles, euhedral garnets (0.1–0.5 mm), anhedral omphacite, clinozoisite and rare corundum (Fig. 10). The kyanite needles have a regular orientation that suggests topotactic nucleation and growth within the plagioclase structure. In some cases, clumps of zoisite/clinozoisite are found in the centers of the plagioclase domains (e.g. Fig. 10). The spatial distribution of the reaction products, i.e. with Ca-rich phases of zoisite and garnet in the cores of the plagioclase and Na-rich omphacite coronas around the rim, probably reflects original igneous zoning in the plagioclase.

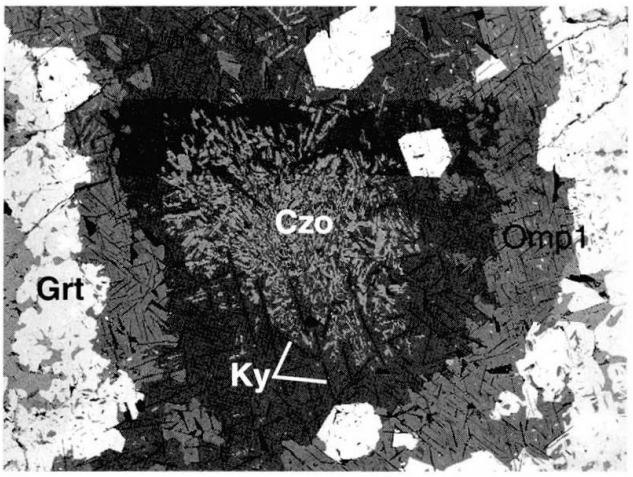

Fig. 10 Back-scattered electron image of plagioclase (darkest grey) and its reaction products from 419952. The texture is produced by the reaction $Pl + H_2O = Jd + Grs + Ky + Zo + NaSiCa_{-1}Al_{-1Pl}$. The image is 11.0 mm wide.

In the presence of water, calcic plagioclase breaks down according to the continuous reaction

$$Pl + H_2O = Ky + Zo + Qtz + (NaSiCa_{-1}Al_{-1})_{Pl} \quad (3)$$

(GOLDSMITH, 1982). The reaction proceeds to the right with increasing pressure leaving behind a more sodic plagioclase. With a further pressure increase omphacite starts to form according to the discontinuous reaction

$$Pl + H_2O = Jd + Ky + Zo + Qtz + (NaSiCa_{-1}Al_{-1})_{Pl} \quad (4)$$

(WAYTE et al., 1989). In the absence of H_2O, the reaction above becomes metastable with respect to the anhydrous breakdown of plagioclase which produces garnet. At anhydrous conditions plagioclase will decompose according to the continuous reaction

$$Pl = Grs + Ky + Qtz + (NaSiCa_{-1}Al_{-1})_{Pl} \quad (5)$$

At higher pressures the terminal breakdown of plagioclase takes place according to the discontinuous reaction

$$Pl = Jd + Grs + Ky + Qtz + (NaSiCa_{-1}Al_{-1})_{Pl} \quad (6)$$

(WAYTE et al., 1989).

The presence of abundant, oriented kyanite needles, not only within the plagioclase, but also within omphacite and garnet (Fig. 10) indicates that kyanite nucleated at an early stage of the plagioclase decomposition. Kyanite and zoisite were most probably produced by reaction (3) during an early stage of the plagioclase breakdown. Further, it can be argued from textural considerations that garnet did not grow before nucleation of omphacite. Instead, the textures suggest that omphacite nucleated *before* or *simultaneously* with garnet. Two possible reaction paths will produce the observed sequence of mineral growth:
i) reaction (3) –> reaction (4) (followed by a decrease in a_{H_2O}) –> reaction (5) and/or (6)
ii) reaction (3) (followed by a decrease in a_{H_2O}) –> reaction (6).

Crystallization of omphacite before garnet implies reaction path i. Kyanite and zoisite may have been produced by reaction (3) during an early stage of the plagioclase breakdown. Increasing pressure will exceed the equilibrium conditions for reaction (4), which produces omphacite in addition to more kyanite, zoisite and quartz. Notice that reaction (4) is not discontinuous, as om-

phacite contains both aegerine-augite and diopside components. The presence of garnet in the plagioclase domain indicates that the system became water undersaturated. Anhydrous breakdown of plagioclase may then have occurred due to reaction (5) or (6).

Simultaneous nucleation of omphacite and garnet implies reaction path ii. Again kyanite and zoisite are produced according to reaction (3). If a_{H_2O} decreased to a critical minimum before the pressure required to cross reaction (4) was attained, then the terminal plagioclase reaction (4) became metastable with respect to reaction (5). Reaction (5) was overstepped without reaction occurring, and finally garnet and omphacite is produced through reaction (6).

The two different reaction pathways are strongly influenced by the activity of water. Reaction (6) is not isochemical because diffusion of Fe and Mg into the plagioclase domains is required in order to crystallize solid solution garnet and the diopside component in omphacite. Additional components to the chemical system have the consequence that reaction (6) becomes continuous. In addition, SiO_2 is released and diffuses out of the plagioclase domains to participate in reaction (2).

BREAKDOWN OF IGNEOUS PYROXENES

Igneous pyroxenes and metamorphic orthopyroxene have coronas composed of diopside and omphacite. The reactions responsible for the transformation from one pyroxene to another involve cation exchange. Omphacite is related to orthopyroxene by the jadeite ($NaAl^{VI}Mg_{-1}Fe_{-1}$), acmite ($NaFe^{3+}Mg_{-1}Fe_{-1}$) and $CaMg_{-1}$ and $CaFe_{-1}$ substitutions, while it is related to diopside by the exchanges $NaAl^{VI}$ <-> CaMg and $NaFe^{3+}$ <-> CaMg. Na and Al are derived from the reactions taking place within the plagioclase domain. Ca, Mg and Fe, which are released by the breakdown of igneous pyroxene, diffuse into plagioclase sites to participate in garnet and omphacite forming reactions. The thin clinopyroxene coronas consisting of omphacite and diopside occur only as transient phases as they are consumed by amphibole producing reactions in the more advanced coronitic stage. The final breakdown of igneous pyroxene does not take place until the amphibolites completely recrystallize. Reactions responsible for formation of amphibole involve extensive diffusion between different chemical domains through a set of complex continuous reactions that might have changed with time.

Estimation of P-T conditions

Peak pressures and temperatures are difficult to estimate for the Ambolten gabbro-norite, since well-equilibrated eclogites were never formed. The obvious chemical and textural disequilibrium negates the derivation of quantitative estimates of metamorphic pressures and temperatures from the coronitic gabbro-norite. However, qualitative estimates can be obtained from phase equilibria arguments and from thermometry on nearby eclogitic rocks. The breakdown of plagioclase to produce the higher density phases kyanite, omphacite and garnet is diagnostic for high-pressure metamorphism. The equilibrium boundary for reaction (6) is roughly located at ≈ 18 kbar at temperatures of 600 °C (WAYTE et al., 1989). Peak pressures probably exceeded 18 kbar at Ambolten because the reaction boundaries were most likely overstepped, and higher temperatures (which shift the reaction curves to higher pressures) were encountered. Garnet-clinopyroxene thermometry (POWELL, 1985 with all Fe as Fe^{2+}) on a nearby retrogressed mafic dike with the assemblage garnet + omphacite + amphibole + biotite + plagioclase + zoisite + rutile (sample 434394) yields peak temperatures of 775–840 °C at 18 kbar. Another retrogressed felsic dike contains garnets with inclusions of omphacite + kyanite + quartz + rutile (sample 434409); temperatures obtained using the same method are 735–775 °C at 18 kbar. Since samples 434394 and 434409 are located only 700 m and 1500 m southeast of the gabbro, respectively, it is reasonable to believe that that gabbro-norite saw similar conditions. The eclogite facies metamorphism at Ambolten is estimated to be in excess of 735 °C and 18 kbar.

Geothermobarometric calculations have also been performed on two samples of well-equilibrated amphibolite (samples 434403 and 434415) from the margin of the gabbro. Metamorphic temperatures and pressures are estimated using garnet-amphibole thermometry (PERCHUK et al., 1985) and garnet-plagioclase-amphibole-quartz barometry (KOHN and SPEAR, 1990). Temperature estimates based on core compositions of garnet and amphibole are 640–670 °C for pressures of 12.5–13.5 kbar.

Discussion

The coronitic textures in the Ambolten gabbro-norite have a marked spatial orientation with a well-defined and systematic sequence of metamorphic mineral zones developed between relict igneous phases. The coronas are themselves

chemically zoned, and pronounced jumps in chemical composition occur at corona boundaries. These features are characteristic of diffusion-controlled structures in metamorphic rocks (FISHER, 1977). The persistence of zoning in the various coronas reflects chemical potential gradients between very different concentrations in the original igneous minerals. Restricted element mobility confines reactions to local domains which in effect allows us to "see through" the metamorphism to the original magmatic textures. Similar diffusion-controlled, high-pressure metamorphic textures have been described in metagabbros from the Alps (CHINNER and DIXON, 1973; POGNANTE, 1985; WAYTE et al., 1989), the Norwegian Caledonides (MØRK, 1985a, 1985b, 1986), the Canadian Grenville Province (INDARES, 1993; INDARES and RIVERS, 1995), and the Sulu UHP Province of China (ZHANG and LIOU 1997). The important variables controlling the corona sequence and reaction products are bulk rock composition, temperature, diffusion rates, fluid availability, and reaction kinetics. No two examples show the same reaction pathways, and this suggests a complex interplay among the important variables.

COMPOSITIONAL EFFECTS

The gabbros studied comprise leucogabbros, gabbro-norites, Fe–Ti rich gabbros; olivine may or may not be part of the igneous mineralogy. POGNANTE (1985) noted that ferro-gabbros were more likely to reequilibrate to eclogites than olivine gabbro-norites in the western Alps. This observation may prove generally true in that eclogite facies reactions go to completion in the ferro-gabbros at Flemsøy (MØRK, 1985a, 1986), at Rocciavré (POGNANTE, 1985), and at Yangkou Beach (ZHANG and LIOU, 1997); whereas, the gabbro-norites at Ambolten, Rocciavré, Kvamsøy (MØRK, 1985b) and in the Canadian Grenville Province (INDARES, 1993; INDARES and RIVERS, 1995) failed to equilibrate. This may reflect the fact that gabbro-norites tend to be poor in bulk Na_2O ($\leq 2\%$).

The chemistry of local domains, particularly plagioclase domains, will also have a strong influence on the reaction pathways. Calcic plagioclase breaks down at lower pressures than sodic plagioclase (GOLDSMITH, 1982; RUBIE, 1990). Zoned magmatic plagioclase would produce particularly complex breakdown pathways. The spatial distribution of reaction products in the plagioclase at Ambolten (Fig. 10) suggests precursor zoning from calcic cores to sodic rims. Plagioclase cores should therefore become unstable before (i.e. at lower pressures) than the rims, and this adds additional complexity to trying to evaluate the reaction history. Igneous plagioclase compositions are seldom recovered from the coronitic gabbros, posing a real problem in evaluating the effect of original chemistry.

EFFECTS OF DIFFUSION AND FLUID INFILTRATION

Eclogites are known to equilibrate over a large range in temperature, i.e. 400–1400 °C (CARSWELL, 1990), and temperature is certainly an important variable for equilibrium predictions of stable assemblages. Higher temperatures enhance diffusion such that one might expect better equilibration at higher T. The Rocciavré (POGNANTE, 1985) and the Allalin (WAYTE et al., 1989) gabbros are low temperature eclogites, but Ambolten and the other examples cited above all saw temperatures in excess of 700 °C. Despite this, the Ambolten and Shabogamo gabbros (INDARES, 1993) never completely transformed to eclogite. High temperature alone is not sufficient to increase diffusion rates.

Many authors cite the lack of a fluid phase as the main factor that hinders equilibration in these partly eclogitized gabbros. In the absence of microcracks, fluids will reside in pockets within grain boundaries and tubules along grain corners (WHITE and WHITE, 1981). The key to whether diffusion is enhanced by fluids may be whether or not the fluids form interconnected channels. WATSON and BRENAN (1987) predict that lower crustal rocks (i.e. $P > 10$ kbar) should contain interconnected fluid channels because of the pressure effects on dihedral wetting angles at grain triple junctions. Evidence of enhanced diffusion at grain corners can be seen in figure 7, where Fe and Mg preferentially diffuse into the corners of relict plagioclase laths to form garnet. Grain boundary diffusion certainly plays a role in mass transfer in the Ambolten gabbro, but is impeded by the coarse grain size.

Equilibrated eclogites are found in the deformed margins of some of the metagabbros (e.g. Flemsøy, Rocciavré and Yangkou). Deformation will enhance diffusion rates by introducing fluids into otherwise dry rocks (e.g. AUSTRHEIM, 1987; AUSTRHEIM and GRIFFIN, 1985; JAMTVEIT et al., 1990) and by increasing the mobility of dislocations during dynamic recrystallization (YUND et al., 1981; OTTEN and BUSECK, 1987; YUND and TULLIS, 1991). But parts of these gabbros, notably Flemsøy, were statically transformed to eclogite.

WATSON and BRENAN'S (1987) model of fluid filled porosity provides a mechanism for fluid-enhanced diffusion that does not require fracturing or plastic deformation.

Interconnected fluid channels can facilitate the transport of cations along grain boundaries, but ultimately lattice diffusion is required to grow the new minerals in the gabbros. For example, plagioclase domains show an amazing diversity of reaction pathways which primarily reflect different lattice diffusion rates amongst the various elements. Plagioclase breakdown is rarely isochemical; garnet and/or omphacite are common reaction products that require diffusion of Fe and Mg into plagioclase to form the almandine and pyrope components of garnet and the diopside component of the omphacite. Even at elevated temperatures, large differences in element mobility are observed. For example, Mg diffusion was extreme at Flemsøy, where tiny spinel laths uniformily cloud plagioclase during an anhydrous transformation to garnet + spinel + sodic plagioclase (MØRK, 1985a, 1986). In comparison, kyanite is abundant and Mg is limited to the pyrope component of garnet at Ambolten. Pseudomorphs of omphacite ± quartz after igneous augite at Flemsøy and Yangkou indicate ready diffusion of Na and Al from plagioclase sites into pyroxene. Na and Al diffusion was much more limited in the Ambolten coronitic gabbros where they were confined to plagioclase domains, or at most leaked out of the plagioclase to form thin omphacite coronas around adjacent pyroxene and olivine grains.

Kinetic barriers to nucleation and growth will also lead to the persistance of metastable phases (WAYTE et al., 1989; RUBIE, 1990), even if lattice diffusion is operating. This is particularly clear for the coesite-bearing Yangkou metagabbro where the anhydrous plagioclase breakdown reaction (6) was overstepped by at least 12 kbar while at the same time K, Fe and Mg were diffusing to plagioclase sites (ZHANG and LIOU, 1997). Reaction (6) was overstepped at Ambolten as well because plagioclase coexists metastably with omphacite (Jd_{35-55}), but the amount of overstep is unknown.

Terrains exhumed from the deep levels of continent-continent collsion zones (i.e 50–100 km) nearly always sustain an amphibolite facies overprint that obscures the nature of the HP metamorphism, especially in the quartzofeldspathic rocks. The partially reacted gabbros described here and elsewhere demonstrate that portions of crust can exist metastably at HP. This is important for two reasons: (1) the partially eclogitized rocks will have a density intermediate between the protolith and the true eclogite, and (2) the overall percentage of crust converted to eclogite determines overall density distribution. The density of the overthickened or subducted crust in collision zones is an important constraint in geodynamic models (AUSTRHEIM, 1991; AUSTRHEIM et al., 1997). The possibility exists that parts of the continental crust remain fairly bouyant even though they have seen HP and UHP conditions. It may be these fragments that are exhumed to the surface rather than submerged into the mantle.

Conclusions

1. Eclogite facies metamorphism of the Ambolten gabbro-norite is demonstrated by the partial replacement of igneous plagioclase by omphacite + garnet + kyanite + zoisite assemblages, the pseudomorphic replacement of olivine by orthopyroxene, and recrystallization of igneous pyroxenes to metamorphic pyroxenes (including omphacite) by a series of coronitic reactions.

2. The preservation of igneous minerals and textures surrounded by coronas of different single phases indicates extreme chemical disequilibriun during diffusion controlled metamorphism.

3. X-ray maps of chemical zoning of major elements within individual phases, especially garnet and clinopyroxene, give a clear picture of element mobility during the high-pressure metamorphism. The compositional zoning reflects chemical potential gradients between unequilibrated metamorphic phases growing between relict igneous mineral domains, rather than changes in external variables (i.e. pressure and temperature).

4. Reaction pathways for plagioclase breakdown are strongly dependent on the activity of the fluid. The persistance of metastable plagioclase in the gabbro-norite at Ambolten suggests low fluid activity during high-pressure metamorphism.

5. Preservation of partly eclogitized, recognizable, mafic intrusive rocks (like the Ambolten gabbro-norite) together with well-equilibrated eclogites within an amphibolite facies, quartzofeldspathic gray gneiss terrain is evidence that the entire terrain was subjected to high pressure conditions. The Ambolten gabbro-norite shares the amphibolite facies exhumation history with its host gneisses, but was more resistant to later deformation and retrograde metamorphism because it stayed dry.

Acknowledgements

The authors are grateful to the National Science Foundation (EAR95–01218) and the Geological Survey of Denmark and Greenland (GEUS) for funding this research. The Ambolten gabbro-norite was discovered by J.M. Hull and J.D. Friderichsen in 1994 during regional mapping for the GEUS sponsored Eastern North Greenland Expedition. We are grateful to G. Rebay and R.Y. Zhang for useful discussions, F. Spear for the use of his Thermobar and Xraymap programs, and H. Austrheim and D.A. Carswell for their helpful reviews. This paper is published with the permission of GEUS.

References

AUSTRHEIM, H. (1987): Eclogitization of lower crustal granulites by fluid migration through shear zones. Earth Planet. Sci. Lett. 81, 221–232.

AUSTRHEIM, H. (1991): Eclogite formation and the dynamics of crustal roots under continental collision zones. Terra Nova 3, 492–499.

AUSTRHEIM, H., ERAMBERT, M. and ENGVIK, A.K. (1997): Processing of crust in the root of the Caledonian continental collision zone: the role of eclogitization. Tectonophysics 273, 129–153.

AUSTRHEIM, H. and GRIFFIN, W.L. (1985): Shear deformation and eclogite formation within granulite-facies anorthosites of the Bergen Arcs, western Norway. Chem. Geol. 50, 267–281.

BIINO, G.G. and COMPAGNONI, R. (1992): Very-high pressure metamorphism of the Brossasco coronite metagranite, southern Dora Maira Massif, Western Alps. Schweiz. Mineral. Petrogr. Mitt. 72, 347–363.

BRUECKNER, H.K., GILOTTI, J.A. and NUTMAN, A. (1998): Caledonian eclogite-facies metamorphism of Early Proterozoic protoliths from the North-East Greenland Eclogite Province. Contrib. Mineral. Petrol., 130, 103–120.

CARSWELL, D.A. (1990): Eclogites and the eclogite facies: definitions and classifications. In: CARSWELL, D.A. (ed.): Eclogite facies rocks. Chapman and Hall, New York, 1–13.

CHINNER, G.A. and DIXON, J.E. (1973): Some high pressure parageneses of the Allalin gabbro, Valais, Switzerland. J. Petrology 14, 185–202.

FISHER, G.W. (1977): Nonequilibrium thermodynamics in metamorphism. In: FRASER, D.G. (ed.): Thermodynamics in Geology. D. Reidel Publishing Company, Dordrecht Holland, 381–403.

GILOTTI, J.A. (1993): Discovery of a medium temperature eclogite province in the Caledonides of North-East Greenland. Geology 21, 523–526.

GILOTTI, J.A. (1994): Eclogites and related high-pressure rocks from North-East Greenland. Rapp. Grønlands geol. Unders. 162, 77–90.

GOLDSMITH, J.R. (1982): Plagioclase stability at elevated temperatures and pressures. Am. Mineral. 66, 1183–1188.

GRIFFIN, W.L. and CARSWELL, D.A. (1985): In situ metamorphism of Norwegian eclogites: an example. In: GEE, D.G. and STURT, B.A. (eds): The Caledonian Orogen – Scandinavia and Related Areas. Wiley, Chichester, 813–822.

HULL, J.M., FRIDERICHSEN, J.D., GILOTTI, J.A., HENRIKSEN, N., HIGGINS, A.K. and KALSBEEK, F. (1994): Gneiss complex of the Skærfjorden region (76–78° N), North-East Greenland. Rapp. Grønlands geol. Unders. 162, 35–51.

INDARES, A. (1993): Eclogitized gabbros from the eastern Grenville Province: textures, metamorphic context, and implications. Can. J. Earth Sci. 30, 159–173.

INDARES, A. and RIVERS, T. (1995): Textures, metamorphic reactions and thermobarometry of eclogitized metagabbros: a Proterozoic example. Eur. J. Mineral. 7, 43–56.

JAMTVEIT, B., BUCHER-NURMINEN, K. and AUSTRHEIM, H. (1990): Fluid controlled eclogitization of granulites in deep crustal shear zones, Bergen Arcs, western Norway. Contrib. Mineral. Petrol. 104, 184–193.

KALSBEEK, F., NUTMAN, A.P. and TAYLOR, P.N. (1993): Palaeoproterozoic basement province in the Caledonian fold belt of North-East Greenland. Precambrian Res. 63, 163–178.

KOHN, M.J. and SPEAR, F.S. (1990): Two new barometers for garnet amphibolites with applications to southeastern Vermont. Am. Mineral. 75, 86–96.

KOONS, P. F. (1987): The effects of disequilibrium on the mineralogical evolution of quartz diorite during metamorphism in the eclogite facies. J. Petrology 28, 679–700.

LEAKE, B.E., WOOLLEY, A.R., ARPS, C.E.S., BIRCH, W.D., GILBERT, M.C., GRICE, J.D., HAWTHORNE, F.C., KATO, A., KISCH, H.J., KRIVOVICHEV, V.G., LINTHOUT, K., LAIRD, J., MANDARINO, J.A., MARESCH, W.V., NICKEL, ROCK, N.M.S., SCHUMACHER, J.C., SMITH, D.C., STEPHENSON, N.C.N., UNGARETTI, L.E.H., WHITTAKER, E.J.W., YOUZHI, G. (1997): Nomenclature of amphiboles: Report of the Subcommittee on Amphiboles of the International Mineralogical Association, Commission on New Minerals and Mineral Names. Am. Mineral. 82, 1019–1037.

MORIMOTO, N., FABRIES, J., FERGUSON, A.K., GINZBURG, I.V., ROSS, M., SEIFERT, F.A., ZUSSMAN, J., AOKI, K., and GOTTARDI, G. (1988): Nomenclature of pyroxenes. Mineral. Mag. 52, 535–550.

MØRK, M.B. (1985a): A gabbro to eclogite transition on Flemsøy, Sunmøre, western Norway. Chem. Geol. 50, 283–310.

MØRK, M.B. (1985b): Incomplete high P-T metamorphic transitions within the Kvamsøy pyroxenite complex, west Norway: a case study of disequilibrium. J. metamorphic Geol. 3, 245–264.

MØRK, M.B. (1986): Coronite and eclogite formation in olivine gabbro (Western Norway): reaction paths and garnet zoning. Mineral. Mag. 50, 417–426.

OBERHÄNSLI, R., HUNZIKER, J.C., MARTINOTTI, G. and STERN, W.B. (1985): Geochemistry, geochronology and petrology of Monte Mucrone: an example of Eo-Alpine eclogitization of Permian granitoids in the Sesia-Lanzo Zone, western Alps, Italy. Chem. Geol. 52, 165–184.

OTTEN, M.T. and BUSECK, P.R. (1987): TEM study of the transformation of augite to sodic pyroxene in eclogitized ferrogabbro. Contrib. Mineral. Petrol. 96, 529–538.

PERCHUK, L.L., ARANOVICH, L.Y., PODLESSKII, K.K., LAVRANT'EVA, I.V., GERASIMOV, V.Y., FED'KIN, V.V., KITSUL, V.I., KARASAKOV, L.P. and BERDNIKOV, N.V. (1985): Precambrian granulites of the Aldan Shield, eastern Siberia, USSR. J. metamorphic Geol. 3, 265–310.

POGNANTE, U. (1985): Coronitic reactions and ductile shear zones in eclogitised ophiolite metagabbro, Western Alps, North Italy. Chem. Geol. 50, 99–109.

POWELL, R. (1985): Regression diagnostic and robust regression in geothermometer/geobarometer calibra-

tion: the garnet-clinopyroxene geothermometer revisited. J. metamorphic Geol. 3, 231–243.

RUBIE, D.C. (1990): Role of kinetics in the formation and preservation of eclogites. In: CARSWELL, D.A. (ed.): Eclogite facies rocks. Blackie, Glasgow, 111–140.

STECHER, O. and HENRIKSEN, N. (1994): Sm–Nd model age of an early Proterozoic gabbro-anorthosite from the Caledonian fold belt in North-East Greenland. Rapp. Grønlands geol. Unders. 162, 135–137.

WATSON, E.B. and BRENAN, J.M. (1987): Fluids in the lithosphere, 1. Experimentally determined wetting characteristics of CO_2–H_2O fluids and their implications for fluid transport, host rock physical properties, and fluid inclusion formation. Earth Planet. Sci. Lett. 85, 496–515.

WAYTE, G.J., WORDEN, R.H., RUBIE, R.C. and DROOP, G.T.R. (1989): A TEM study of disequilibrium plagioclase breakdown at high pressure: the role of the infiltrating fluid. Contrib. Mineral. Petrol. 101, 426–437.

WHITE, J.C. and WHITE, S.H. (1981): On the structure of grain boundaries in tectonites. Tectonophysics 78, 613–628.

YUND, R.A., SMITH, B.M. and TULLIS, J. (1981): Dislocation-assisted diffusion of oxygen in albite. Phys. Chem. Minerals 7, 185–189.

YUND, R.A. and TULLIS, J. (1991): Compositional changes of minerals associated with dynamic recrystallization. Contrib. Mineral. Petrol. 108, 346–355.

ZHANG, R.Y. and LIOU, J.G. (1997): Partial transformation of gabbro to coesite-bearing eclogite from Yangkou, the Sulu terrane, eastern China. J. metamorphic Geol., 15, 183–202.

Manuscript received October 2, 1997; revision accepted March 10, 1998.